

# Nonlinear resonance reflection from and transmission through a dense glassy system built up of oriented linear Frenkel chains:

## Two-level model

E. Conejero Jarque

*Departamento de Física Aplicada, Universidad de Salamanca, E-37008 Salamanca, Spain*

V. A. Malyshev

*National Research Center "Vavilov State Optical Institute", Birzhevaya Liniya 12, 199034*

*Saint-Petersburg, Russia*

(October 26, 2018)

### Abstract

A theoretical study of the resonance optical response of assemblies of oriented short (as compared to an optical wavelength) linear Frenkel chains is carried out. Despite the fact that the energy spectrum of a single chain is composed of the bands of Frenkel exciton states, a two-level model is used to describe the optical response of a single linear chain. We account for only the (on-resonance) optical transition between the ground state and the state of the one-exciton band bottom as having the dominating oscillator strength as compared to the other states of the one-exciton manifold. The (off-resonance) process of creation of two excitons per chain is neglected because it requires a higher excitation frequency due to the quasi-fermionic nature of one-dimensional Frenkel excitons. A distribution of linear chains over length resulting in fluctuations of all exciton optical parameters, such as the transition frequency and dipole moment as well as the radiative rate, are

taken explicitly into account.

We show that both transmittivity and reflectivity of the film may behave in a bistable fashion, originated from saturation of the nonlinear refraction index, and analyze how the effects found depend on the film thickness and on the inhomogeneous width of the exciton optical transition. Estimates of the driving parameters show that films of oriented J-aggregates of polymethine dyes at low temperatures seem to be suitable species for the experimental verification of the behavior found.

PACS number(s): 42.65.Pc, 78.66.-w

## I. INTRODUCTION

Since pioneering works of Jelley<sup>1</sup> and Scheibe<sup>2</sup>, who discovered the phenomenon of linear aggregation of polymethine dye molecules in solution with rising their volume concentration and, as a result, drastic changes of their optical properties (the appearance of a red-shifted narrow band, called now J-band), these species have been the subject of unremitting interest of reseachers. In the beginning of the nineties, Wiersma and co-workers<sup>3–5</sup> demonstrated the possibility of further narrowing of the J-band as well as shortening of its emission lifetime by an order of magnitude via cooling to the temperature of liquid helium. At present, it is widely accepted that the unusual properties of such systems originate from the fact that their optically active states are Frenkel exciton states (see for a comprehensive review Refs. 6 and 7).

In recent time, a considerable attention has been drawn to the problem of strong coupling of organic polymers and molecular aggregates to resonant radiation. Room temperature spectral narrowing of emission<sup>8,9</sup> and cooperative emission<sup>10,11</sup> in  $\pi$ -conjugated polymer thin films, superradiant lasing from the J-aggregated cyanine dye molecules adsorbed onto colloidal silica and silver<sup>12,13</sup> as well as the room temperature polariton emission from strongly coupled organic semiconductor microcavities<sup>14</sup> have been reported. All these effects unambiguously mean a collectivization of polymers and J-aggregates via the emission field and are of great importance from the viewpoint of laser applications (see Refs. 15–17 for reviews). On the other hand, the conditions of such a strong coupling are those necessary for manifestation of a bistable behavior of a collection of homogeneously broadened two-level systems.<sup>18–23</sup> Much efforts have been undertaken to this problem with its projection to J-aggregated assemblies. The conditions for the bistable optical response to observe from an individual J-aggregate<sup>24–27</sup> and even of a dimer<sup>24,28–30</sup> have been analyzed. Bistability discussed in Refs. 24–27,30 is attributed to *an individual* aggregate and consists of an abrupt switching of the aggregate population from a low level to a higher one as the pump intensity rises. Consequently, the reflectivity (transmittivity) of a macroscopic ensemble of such

species may be switched off (on) in a step-wise way, allowing thus creation of an all-optical bistable element.

The effect we are speaking about originates from the dynamical resonance frequency shift dependent on the population of the system. However, as it has been shown in Refs. 25,27 and 30, an aggregate of a length smaller than the emission wavelength does not display any bistable behavior. This finding makes the above mechanism of the aggregate bistability to be hardly experimentally verified. Indeed, despite an aggregate may incorporate to itself thousands of molecules and thus may have a length larger than the emission wavelength, in reality, only a subsystem of segments, consisting of a portion of the aggregate (the so-called coherently bound molecules), responds to the action of a resonant external field.<sup>31</sup> Because of a disorder (of static and thermal nature) of the surroundings, the exciton coherence length, being the physical length of an aggregate in the absence of disorder, is reduced to a size  $N^*$  dependent on the degree of disorder. For the real conditions, the number  $N^*$  is usually smaller than the emission wavelength counted in the lattice unit. At room temperature,  $N^*$  is determined basically by dephasing (originated from thermal fluctuations of molecular positions) and has an order of magnitude of several lattice units.<sup>32,33</sup> On decreasing the temperature, disorder tends to be of static nature. It is determined by static fluctuations of the aggregate structure as well as the surroundings and becomes dominating as the temperature approaches zero. The static disorder results in Anderson localization of the exciton within an aggregate segment with the typical size of the order of several tens of lattice units.<sup>3-5,34,35</sup> The number of molecules within the localization length plays now the role of  $N^*$  and, in fact, represents a higher limit for the number of coherently bound molecules. Further increasing  $N^*$  would be possible by means of reducing the degree of static disorder that is generally out of control.

In this connection, in Refs. 36 the question was risen whether *an ensemble* of localized exciton states may behave in a bistable fashion. It was used the fact that the exciton states, located within the same localization domain and being active in the optical response, form a local energy structure with a few levels (two or three) similar to the one existing on a regular

chain with length  $N \sim N^*$ .<sup>37,38</sup> In other words, an aggregated sample can be modelled by an ensemble of short (compared to the emission wavelength) linear Frenkel chains stochastically distributed over their lengths  $N$ . It was shown that an ultrathin film with a thickness much smaller than the emission wavelength (which makes possible to use the mean-field approach) manifested bistability of the resonance optical response.

In this paper, we follow the conjecture proposed in Refs. 36 and generalize the results reported there to film thicknesses of the order of or larger than the emission wavelength, when the mean-field approach, being an adequate approximation for thinner films, is no longer valid. This paper is organized as follows. In Sec. II, we present the model and mathematical formalism. Section III deals with an analysis of the feasibility of a bistable response from an ultrathin film (under the condition of validity of the mean field approximation), taking into account the fluctuations of all exciton optical parameters, such as the one-exciton transition frequency and dipole moment as well as the one-exciton exciton radiative rate.<sup>39</sup> Further (Sec. IV), we present results of numerical simulations for thin films of thickness larger than the emission wavelength and determine the ranges of driving parameters, for which the film reflectivity and transmittivity manifests bistability. In Sec. V, we make estimates for J-aggregates of PIC and show that critical parameters for the occurrence of such a behavior seems to be achievable for thin films at low temperatures. Finally, Sec. VI concludes the paper. Some preliminary results of the present study have been reported in our recent paper.<sup>40</sup>

## II. DESCRIPTION OF THE MODEL

An elementary object of an ensemble we will be dealing with represents a short (with a length smaller than the emission wavelength) ordered linear chain consisting of  $N$  two-level molecules (with  $N$  much larger than unity). Due to the strong intermolecular dipolar coupling, the optically active states are the Frenkel exciton states rather than the states of individual molecules. In the nearest-neighbour approximation, which we adopt hereinafter,

one-dimensional Frenkel excitons appear to be non-interacting fermions<sup>41</sup> so that any state with a fixed number of excitons can be constructed as a Slater determinant of one-exciton states

$$|k\rangle = \left(\frac{2}{N+1}\right)^{1/2} \sum_{n=1}^N \sin \frac{\pi kn}{N+1} |n\rangle, \quad k = 1, 2, \dots, N, \quad (1)$$

where  $|n\rangle$  is the ket-vector of the excited state of the  $n$ th molecule. The energies of the one-dimensional exciton gas may take the values  $W = \sum_{k=1}^N n_k E_k$ , where  $n_k = 0, 1$  is the occupation number of the  $k$ th one-exciton state and  $E_k$  is the corresponding energy given by

$$E_k = \hbar\omega_{21} - 2U \cos \frac{\pi k}{N+1}, \quad (2)$$

where  $\omega_{21}$  is the transition frequency of an isolated molecule and  $U$  (chosen hereinafter to be positive) is the magnitude of the nearest-neighbour hopping integral.

The optical transition from the ground state of the chain to the lowest state of the one exciton band  $k = 1$  has the dominating oscillator strength (81% of the total one; see, for instance, Ref. 6). Furthermore, the transition between the bottoms of one-exciton and two-exciton bands is blue-shifted as compared to the ground-state-to-one-exciton band bottom transition by an energy  $E_2 - E_1 = 3\pi^2 U/N^2$ . The blue shift originates of the fermionic nature of one-dimensional Frenkel excitons and was experimentally verified for the first time in Ref. 42. These two facts were put forward in Ref. 36 as a motivation to consider the transition from the ground state to the bottom of the one-exciton band as an isolated two-level transition. This assumption can indeed be approved provided that the actual Rabi frequency of the external field is smaller than the blue shift of one-to-two exciton transitions. Further analysis of the transitions to higher exciton manifolds showed that they did not lead to qualitative changes of the behavior found within the framework of the two-level model.<sup>43</sup> Based on these findings and taking into account that the spatial inhomogeneity of the field and matter variables complicates the treatment drastically, we will use in what follows the two-level approach to describe the matter response.

Thus, we model the ensemble of linear Frenkel chains as that comprised of inhomogeneously broadened (due to the fluctuations of chain lengths) two-level systems, but with the optical characteristics of the transition having all attributes of a one-exciton transition. Note that neglecting the one-to-two-exciton optical transitions means that no more than one exciton per chain is created by the external field. Respectively, such a channel of efficient exciton quenching as the intra-chain exciton-exciton annihilation<sup>44</sup> plays no role within the framework of the two-level approximation. In principle, the excitonic annihilation can involve two excitons created on different chains. As follows, however, from the results presented in Ref. 44, the rate of such a process is negligible under the restrictions of our model: low temperature and  $N \gg 1$ .

We also assume that the transition dipole moments of all chains are parallel to each other as well as to the film plane.<sup>45</sup> With regard to the input field  $\mathcal{E}_i$ , the on-resonance and normal incidence conditions are chosen. The input field polarization can be set without loss of generality to be directed along the transition dipole moment. Then, all quantities can be considered as scalars.

Under the above limitations, the time evolution of the film is described in terms of the  $2 \times 2$  density matrix  $\rho_{\alpha\beta}$  ( $\alpha, \beta = 1, 2$ ) standing for determination of the state of a chain of length  $N$ . The density matrix equation together with the Maxwell equation for the total field  $\mathcal{E}$ , including a secondary field produced by the film, form the closed system of equations in the problem we are dealing with. It reads

$$\dot{\rho}_{21} = -(i\omega + \Gamma)\rho_{21} - i\frac{d\mathcal{E}}{\hbar}Z, \quad (3a)$$

$$\dot{Z} = 2i\frac{d\mathcal{E}}{\hbar}[\rho_{12} - \rho_{21}] - \Gamma_1(Z + 1), \quad (3b)$$

$$\mathcal{E}(x, t) = \mathcal{E}_i(x, t) - \frac{2\pi}{c} \int_0^L dx' \frac{\partial}{\partial t} \mathcal{P} \left( x', t - \frac{|x - x'|}{c} \right). \quad (3c)$$

where the dots denote time derivatives;  $Z = \rho_{22} - \rho_{11}$ ;  $\omega = \omega_{21} - 2(U/\hbar) \cos[\pi/(N + 1)] \approx \omega_{21} - 2U/\hbar + U\pi^2/\hbar N^2$  is the transition frequency for an individual chain of size  $N$ ;  $d$  is

the transition dipole moment of a chain of size  $N$  scaled as  $d = d_0\sqrt{N}$ , where  $d_0$  is the transition dipole moment for an isolated molecule;  $\Gamma_1$  is the spontaneous emission constant of the optically active one-exciton state:  $\Gamma_1 = \gamma_0 N$  with  $\gamma_0$  being the analogous constant for an isolated molecule (for the sake of simplicity, we have replaced the numerical factor  $8/\pi^2$  in the expression for  $d$  and  $\Gamma_1$  by unity);  $\Gamma = \Gamma_1/2 + \Gamma_2$  is the dephasing constant including the contribution ( $\Gamma_2$ ) not connected with the radiative damping.

The last formula of the set (3) is nothing else but the integral form of the Maxwell equation for a film, in which  $c$  and  $L$  stand for the speed of light and for the film thickness, respectively, and  $\mathcal{P}$  is the electric polarization:

$$\mathcal{P} = n_0 \langle d(\rho_{21} + \rho_{12}) \rangle, \quad (4)$$

where  $n_0$  is the volume density of chains in the film and the angle brackets denote averaging over the chain length distribution with a probability distribution function  $p(N)$ :  $\langle \dots \rangle \equiv \sum_N p(N) \dots$

As was pointed out in Refs. 21,22,47–51, using the integral wave equation to study the non-stationary nonlinear response from a dense absorber has an obvious advantage: the boundary conditions are not required within this framework. Indeed, the reflected  $\mathcal{E}_r = \mathcal{E}(0, t) - \mathcal{E}_i(0, t)$  and transmitted  $\mathcal{E}_{tr} = \mathcal{E}(L, t)$  fields can be calculated obviously on the basis of Eq.(3c) if the spatial distribution of the electric polarization  $\mathcal{P}$  is known. The latter, in turn, is calculated from constituent equations (3a) - (3b) and (4). The background refraction index is not included in Eq.(3c) because, in fact, this simply results in constant renormalization.<sup>49</sup>

Rigorously speaking, for a dense system as that we are considering, the deviation of the acting field from the average (Maxwell) field may be significant. A simplest way to account for this difference is to add the (Lorentz-Lorenz) local-field correction in the form  $(4\pi/3)\mathcal{P}$  to the Maxwell field  $\mathcal{E}$  in the matter equations (3a)-(3b) (see, for instance, Ref. 21). Along this paper, however, we will neglect the local field correction justifying this approximation by our previous study: for that arrangement of the incident frequency we are going to study



(see Sec. IV B), this correction leads only to small quantitative effects.<sup>49</sup>

Assume that the incident field has the form  $\mathcal{E}_i = E_i(t) \cos(\omega_i t - k_i x)$ , where  $\omega_i$  and  $k_i = \omega_i/c$  are the frequency and wavenumber, respectively, and  $E_i(t)$  is the amplitude, slowly varying in the scale of the optical period  $2\pi/\omega_i$ . Thus, by passing to the rotating frame by means of the representation  $\rho_{21} = -(i/2)R \exp(-i\omega_i t)$  and  $\mathcal{E} = (1/2)E \exp(-i\omega_i t) + c.c.$ , with complex amplitudes  $R$  and  $E$  slowly varying in time, and neglecting the counter-rotating terms, we obtain the set of truncated equations

$$\dot{R} = -(i\Delta + \Gamma)R + \frac{dE}{\hbar}Z, \quad (5a)$$

$$\dot{Z} = -\frac{d}{2\hbar}(ER^* + E^*R) - \Gamma_1(Z + 1), \quad (5b)$$

$$E(x, t) = E_i \left( t - \frac{x}{c} \right) e^{ik_i x} + 2\pi n_0 k_i \int_0^L dx' e^{ik_i |x-x'|} \left\langle dR \left( x', t - \frac{|x-x'|}{c} \right) \right\rangle, \quad (5c)$$

Here, the notation  $\Delta = \omega - \omega_i$  is introduced.

The reflected and transmitted waves we are interested in are simply given by the formulae:

$$E_r(t) = E(0, t) - E_0(t) = 2\pi k_i n_0 \int_0^L dx e^{ik_i x} \left\langle dR \left( x, t - \frac{x}{c} \right) \right\rangle. \quad (6a)$$

$$E_t(t) = E(L, t) = \left[ E_i(t) + 2\pi k_i n_0 \int_0^L dx e^{-ik_i x} \left\langle dR \left( x, t - \frac{L-x}{c} \right) \right\rangle \right] e^{ik_i L}. \quad (6b)$$

As in our previous papers,<sup>48-50</sup> we will neglect the retardation effects replacing  $t - |x - x'|/c$  by  $t$  since the film thickness of our interest is of the order of a few vacuum wavelengths,  $\lambda_i = 2\pi/k_i$ . Thus, the actual passage time of the light through the film has the order of magnitude of the optical period while all the characteristic times of the problem discussed ( $\Gamma$ ,  $\hbar/dE_i$ ,  $\Delta^{-1}$ ) are much longer. One can, therefore, consider the field as propagating instantaneously inside the film.

To perform numerical calculations, let us rewrite Eqs. (5) in a dimensionless form using the dimensionless field amplitudes  $e = \bar{d}E/\hbar\bar{\Gamma}$  and  $e_i = \bar{d}E_i/\hbar\bar{\Gamma}$  as well as the dimensionless

spatial and temporal coordinates  $\xi = k_i x$  and  $\tau = \bar{\Gamma} t$ , where  $\bar{d} = \langle d \rangle$  and  $\bar{\Gamma} = \langle \Gamma \rangle$  are the mean transition dipole moment and the mean relaxation constant, respectively. One thus gets

$$\dot{R} = -(i\delta + \gamma)R + \mu e Z , \quad (7a)$$

$$\dot{Z} = -\frac{1}{2}\mu(eR^* + e^*R) - \gamma_1(Z + 1) , \quad (7b)$$

$$e(\xi, \tau) = e_i(\tau)e^{i\xi} + \Psi \int_0^{k_i L} d\xi' e^{i|\xi - \xi'|} \langle \mu R(\xi', \tau) \rangle , \quad (7c)$$

$$e_r(\tau) = \Psi \int_0^{k_i L} d\xi e^{i\xi} \langle \mu R(\xi, \tau) \rangle , \quad (7d)$$

$$e_t(\tau) = \left[ e_i(\tau) + \Psi \int_0^{k_i L} d\xi e^{-i\xi} \langle \mu R(\xi, \tau) \rangle \right] e^{ik_i L} , \quad (7e)$$

where  $\delta = \Delta/\bar{\Gamma}$  ,  $\gamma = \Gamma/\bar{\Gamma}$  ,  $\mu = d/\bar{d}$  ,  $\gamma_1 = \Gamma_1/\bar{\Gamma}$  , and  $\Psi = 2\pi d^2 n_0 / \hbar \bar{\Gamma}$  .

In our simulations, we choose as distribution function  $p(N)$  a Gaussian centered around  $\bar{N}$  with standard deviation  $a$

$$p(N) = \frac{1}{\sqrt{2\pi}a} \exp \left[ -\frac{(N - \bar{N})^2}{2a^2} \right] , \quad (8)$$

assuming  $a < \bar{N}$ . Under this assumption, it is easy to show that the distribution function of the detuning  $\delta$  also presents a Gaussian centered at  $\delta_0 = (\omega_{21} - 2U/\hbar + U\pi^2/\hbar\bar{N}^2 - \omega)/\bar{\Gamma}$  with standard deviation  $\sigma = 2\pi^2 U a / \hbar \bar{\Gamma} \bar{N}^3$ . The quantity  $\sigma$  can be identified with the inhomogeneous width of the exciton absorption line, so that the limits  $\sigma \ll 1$  and  $\sigma \gg 1$  (or  $2\pi^2 U a / \hbar \bar{N}^3 \ll \bar{\Gamma}$  and  $2\pi^2 U a / \hbar \bar{N}^3 \gg \bar{\Gamma}$  in dimensional units) correspond to the cases of dominating homogeneous and inhomogeneous broadening, respectively.

Equations (7) constitute the basis of our analysis of the optical response from a thin film consisting of linear Frenkel chains. We will be interested in the reflection and transmission coefficients for amplitude, which are given by  $\mathcal{R} = \left| [e(0, \tau) - e_i(0, \tau)] / e_i(0, \tau) \right|$  and  $\mathcal{T} = \left| e(k_i L, \tau) / e_i(k_i L, \tau) \right|$ .

### III. ULTRATHIN FILM, $L < \lambda'$

We turn first to the case of an ultrathin film ( $L < \lambda'$  with  $\lambda'$  being the wavelength inside the film) when the spatial dependence of  $R$  and  $Z$  can be neglected and the exponentials in Eq. (7c) can be replaced by unity inside the film. Then, equations for the fields are simplified drastically:

$$e(\tau) = e_i(\tau) + \psi \langle \mu R(\tau) \rangle , \quad (9a)$$

$$e_r(\tau) = \psi \langle \mu R(\tau) \rangle , \quad (9b)$$

$$e_t(\tau) = e_i(\tau) + \psi \langle \mu R(\tau) \rangle , \quad (9c)$$

where  $\psi = \Psi k_i L$ .

First of all, we are interested in the stationary states in which the system can be found. This implies to look for steady-state solutions to Eqs. (7), i.e., letting  $\dot{R} = \dot{Z} = 0$ . Under the simplification (9), valid for an ultrathin film, it is straightforward to arrive to a closed equation for the transmission coefficient  $\mathcal{T}$ :

$$\begin{aligned} \mathcal{T}^2 \left[ \left( 1 + \psi \left\langle \mu^2 \frac{\gamma}{\delta^2 + \gamma^2 + \mu^2 e_i^2(\gamma/\gamma_1) \mathcal{T}^2} \right\rangle \right)^2 \right. \\ \left. + \psi^2 \left\langle \mu^2 \frac{\delta}{\delta^2 + \gamma^2 + \mu^2 e_i^2(\gamma/\gamma_1) \mathcal{T}^2} \right\rangle^2 \right] = 1 . \end{aligned} \quad (10)$$

Whenever  $\mathcal{T}$  is found, the reflection coefficient  $\mathcal{R}$  can be expressed through  $\mathcal{T}$  as follows:

$$\begin{aligned} \mathcal{R}^2 = \psi^2 \left[ \left\langle \mu^2 \frac{\gamma}{\delta^2 + \gamma^2 + \mu^2 e_i^2(\gamma/\gamma_1) \mathcal{T}^2} \right\rangle^2 \right. \\ \left. + \left\langle \mu^2 \frac{\delta}{\delta^2 + \gamma^2 + \mu^2 e_i^2(\gamma/\gamma_1) \mathcal{T}^2} \right\rangle^2 \right] \mathcal{T}^2 . \end{aligned} \quad (11)$$

In absence of the chain length fluctuations, Eq. (10) is of third order with respect to  $\mathcal{T}^2$  and thus may have three real roots,<sup>36</sup> indicating the possibility of bistable behavior of the system

transmittivity. It occurs at  $\psi > \psi_c = 8$ . Due to the relation (11), the system reflectivity is expected to behave in the same manner. The chain length fluctuations make in general impossible to predict the order of the resulting (after carrying out the averaging procedure) transcendent equation.

In Ref. 36, Eq. (10) was analyzed under the assumption that the main effect of the length fluctuations originates in the distribution of detuning  $\delta$ , while fluctuations of the rest of parameters ( $\mu$ ,  $\gamma$ ,  $\gamma_1$ ) are of no importance. Replacing then the distribution over length,  $p(N)$ , by a distribution over detuning and taking the latter in the form of a Lorentzian of width  $g$ , authors of Ref. 36 could evaluate integrals in Eq. (10) analytically and found that the resulting equation gives rise to a bistable behavior, even under the condition of dominating inhomogeneous broadening ( $g > \gamma$ ).

Here, we do not restrict ourselves to the above assumption and carry out calculations, accounting for fluctuations of all stochastic variables in Eq. (10). We present the results for a particular case of the incident frequency tuned up to the center of the absorption band ( $\delta_0 = 0$ ). Figure 1 shows a "phase" diagram of the system behavior in the space of parameters ( $\sigma$ ,  $\psi$ ) calculated on the basis of Eq. (10). The parameters of Gaussian  $p(N)$  were chosen as  $\bar{N} = 30$  and  $a = 9$ . By the terms "one solution" and "three solutions" in Fig. 1, we marked regions where Eq. (10) had single-valued and three-valued real solutions, respectively. The solid curve, which separates these two regions, is nothing but the critical value of  $\psi$  for bistability to occur versus the inhomogeneous width  $\sigma = 2\pi^2 U a / \hbar \bar{\Gamma} \bar{N}^3$ . It starts from  $\psi_c = 8$  at  $\sigma = 0$ , in full correspondence with the earlier findings,<sup>18,19,36</sup> and then gradually goes up on increasing  $\sigma$ .

For comparison, we also depicted in Fig. 1 the curve (dashed) obtained under the approximations used in Ref. 36, i.e., assuming the detuning  $\delta$  as being the unique stochastic variable and setting  $\mu = \gamma = 1$ ,  $\gamma_1 = \text{const}$ . As can be seen, there is almost no difference between the solid and dashed curves. This means that indeed, fluctuations of the detuning basically determine the result of averaging in Eq. (10), thus approving this heuristic assumption used in Ref. 36.

Figure 2 presents the typical examples of the input field dependence of the reflection and transmission coefficients for an ultrathin film ( $k_i L = 0.1$ ) which were obtained by the numerical solution of Eqs. (7) at adiabatic scanning of the input field amplitude  $e_i$  up and down. The results were obtained choosing the following set of parameters:  $\psi = 20$ ,  $\bar{N} = 30$ ,  $a = 9$ ,  $\gamma_1 = 0.25N/\bar{N}$ ,  $\gamma = 0.875 + 0.125N/\bar{N}$ . From this figure, one can conclude that, when the inhomogeneous width  $\sigma$  is small, the system shows a stable hysteresis loop (optical hysteresis) both in reflectivity and transmittivity, despite the fact that fluctuations of all parameters are taken into account (note that the hysteresis of transmittivity in Ref. 36 was calculated only for the particular case of absence of the chain length fluctuations). However, as  $\sigma$  grows, the hysteresis cycle disappears and only a one-valued monotonic response exists.

In order to gain insight into the time required for the output signal to approach its stationary value, we have numerically solved Eqs. (7) at a fixed amplitude of the input field,  $e_i$ , and its further step-wise switching to another value. Figure 3 shows an example of such calculations for the same set of parameters as in Fig. 2, setting  $\sigma = 0.25$ . We start with a non-saturating incident field amplitude  $e_i = 3$ , for which the reflection (transmission) coefficient is high (low), and wait for a stationary value of the latter. At some instant of time (in particular, at  $\tau = \bar{\Gamma}t = 50$ ), we switch step-wisely the incident field to a saturating value  $e_i = 6$ , for which the reflection (transmission) coefficient is low (high), and wait again for a stationary value of the latter. The results of these calculation are depicted in Fig. 3 with solid lines. With dotted lines, we present the results of analogous calculations obtained only by switching back the incident field amplitude from a higher ( $e_i = 6$ ) to a lower ( $e_i = 3$ ) value.

From these data, it can be claimed first that the transient time depends on whether the incident field amplitude is switched up or down. Second, the transient time is of the order of a few units of the population relaxation time  $\bar{\Gamma}_1^{-1}$ . Indeed, in units of  $\bar{\Gamma}^{-1}$  this time interval is of the order of 10. Taking into account that  $\bar{\Gamma}_1/\bar{\Gamma} = 0.25$  in this particular calculation, one arrives at the above stated conclusion.

## IV. THICK FILM, $L > \lambda'$

### A. Motivation

In our previous studies of nonlinear resonant reflection from an extended ( $L > \lambda'$ ) dense system of *homogeneously broadened* two-level molecules,<sup>48–50</sup> we found that the reflectivity of such a system could show different regimes (bistability and self-oscillations<sup>48,49</sup> as well as chaos<sup>50</sup>) basically governed by the parameter  $\Psi$ , instead of  $\psi = \Psi kL$  for an ultrathin film (see also Refs. 52,53). The physical meaning of  $\Psi$  is nothing but the halfwidth (in units of the homogeneous width  $\bar{\Gamma}$ ) of a gap in the spectrum of field + molecules collective excitations - polaritons (polariton splitting; see for more details the monograph by Davydov 54). This gap appears in the vicinity of the molecule-field resonance and requires the condition  $\Psi \gg 1$  to be fulfilled. The linear dielectric constant for frequencies ranging within the gap is negative (the refractive index is imaginary), implying total reflection of the light of such frequencies.<sup>54</sup>

The physical origin of the effects reported in Refs. 48–50,53 is attributed to saturation of the refraction index by the field acting within the polariton band gap. Let us recall briefly the motivation rised in those papers. For an input field varying slowly in the scale of the relaxation times  $\Gamma^{-1}, \Gamma_1^{-1}$  (the case of our interest in the present study), the medium adiabatically follows the field ( $\dot{R}$  can be set to zero). Under such conditions, Eqs. (7a) and (7c) are equivalent to only one equation:<sup>48,49</sup>

$$\frac{d^2 e}{d\xi^2} + \varepsilon(|e|^2)e = 0, \quad (12a)$$

$$\varepsilon(|e|^2) = 1 + 2\Psi \left\langle \mu \frac{i\gamma + \delta}{\gamma^2 + \delta^2 + \mu^2 |e|^2 \gamma / \gamma_1} \right\rangle, \quad (12b)$$

The quantity  $\varepsilon(|e|^2)$  is the field-dependent dielectric function in which fluctuations of all parameters ( $\mu, \gamma, \gamma_1, \delta$ ) are explicitly taken into account. The limit of absence of the chain length fluctuations ( $\mu = \gamma = 1, \gamma_1 = \text{const}$  and  $\delta = \text{const}$ ) formally corresponds to the case considered in Refs. 48–50,53:

$$\varepsilon(|e|^2) = 1 + 2\Psi \frac{i + \delta}{1 + \delta^2 + |e|^2/\gamma_1} . \quad (13)$$

We assume now that  $\Psi \gg 1$  and neglect for a moment the field (linear case). Then, as can be seen from Eq. (13), the linear dielectric function  $\varepsilon$  has a dominating negative real part within a rather wide interval of changing the detuning, in fact, from a few negative units to  $-2\Psi$ . A weak field acting within this band will be totally reflected from the system boundary. At higher amplitudes of the field,  $\gamma|e|^2/\gamma_1 \gg \Psi$ , the dielectric function is saturated by the acting field, i.e., goes to unity, producing conditions for penetration of the field into the medium. The higher the field amplitudes, the deeper the field penetrates into the medium. Now, reflection occurs from a very narrow (due to a high magnitude of  $\Psi$ ) interface between the saturated and non-saturated regions.<sup>52</sup> This interface plays the role of an "artificial" mirror giving rise to a feedback necessary for the effects outlined above to build up.

It turned out that namely in the limit of larger  $\Psi$ , i.e., in the presence of the polariton band gap, the system shows the above mentioned peculiarities of nonlinear optical response that are absent in the opposite case  $\Psi \leq 1$ . When inhomogeneous broadening dominates (the main range of our interest), one should compare the inhomogeneous width  $2\sigma$  with the width of the gap  $2\Psi$ . A simple analysis of Eq. (12b) reveals the clear result that a well-pronounced gap (where the dielectric function has a dominating negative real part) develops at  $\Psi \gg \sigma$ . An inhomogeneous broadening of the order of, or higher than  $2\Psi$  destroys the gap and, as a consequence, all the nonlinear effects accompanying the presence of this gap. Below, we show details of the influence of inhomogeneous broadening on the nonlinear optical response of the film.

## B. Numerical simulations and discussions

All nonlinear features accompanying the presence of the polariton gap were found to be stronger when the input field frequency lies in the middle of the gap, i.e., at  $\delta = -\Psi$ .<sup>48–50,53</sup> Therefore, when studying the nonlinear reflection from and transmission through a film consisting of *inhomogeneously broadened* two-level systems, we will also set  $\delta = -\Psi$  and

consider  $\Psi > \Psi_c = 4.66$  ( $\Psi_c$  is the threshold for bistability in reflection<sup>48</sup>) to get the optimal conditions for the effects we are looking for. It is worth noting that, as was found in Ref. 49, the local-field correction at  $\delta = -\Psi$  has a relatively small quantitative effect. In particular, the threshold value  $\Psi_c$  changes from 4.66 to 5.45 if the local-field correction is taken into account.

Figure 4 presents examples of the input field dependence of the reflection and transmission coefficients for a thin film of thickness  $L = \lambda_i$  depending on the inhomogeneous width  $\sigma = (2\pi^2 a / \bar{N}^3) \cdot (U / \hbar \bar{\Gamma})$ , where  $\bar{N}$  and  $a$  were fixed ( $\bar{N} = 30$ ,  $a = 9$ ) and  $U / \hbar \bar{\Gamma}$  was varied. The other parameters were chosen as follows:  $\Psi = -\delta = 6$ ,  $\gamma_1 = 0.25N / \bar{N}$ ,  $\gamma = 0.875 + 0.125N / \bar{N}$ . The data were obtained at adiabatic scanning of the input field amplitude  $e_i$  up and down. From this figure, one can conclude, first, that the system shows a stable hysteresis loop both in reflectivity and in transmittivity or, in other words, behaves in a bistable fashion until  $\sigma < \Psi$ , i.e., until the inhomogeneous width approaches the polariton splitting, in full correspondence with what we mentioned above. The second observation, evident from Fig. 4, is that the switching amplitudes of the input field do not depend strongly on the inhomogeneous width (at a fixed magnitude of  $\Psi$ ).

In Fig. 5, we depicted spatial profiles of the amplitude module of the field inside the film versus the input field amplitude  $e_i$ . The calculations were performed for the same set of parameters and conditions as those presented in Fig. 4, only setting  $\sigma = 2$ . Plots (a) and (b) correspond to adiabatic scanning of  $e_i$  up and down, respectively. The darkness of a local differential domain is proportional to the field amplitude module. Observing these plots, we can claim the following. Despite the fact that the thickness of the system does not exceed one wavelength in vacuum,  $\lambda_i$ , the field inside the film is not uniform at any amplitude of the input field. For not-saturating magnitudes of  $e_i$ , this is simply explained by the fact that the (linear) refraction index in this case (at  $\delta = -\Psi$ )  $n \approx -1$ , that, in turn, gives rise to decreasing the field amplitude on a scale short compared to  $\lambda_i$ . At higher magnitudes of the input field, ranging within the bistable interval (see Fig. 4), the spatial inhomogeneity of the field demonstrates a global character, originating in the interplay between the forward



and backward (in the present case, reflected from the back boundary of the film) waves.

Comparison of the field profiles depicted in the plots (a) and (b) at a fixed magnitude of the input field reveals that they differ one from the other. In other words, one may make a statement about the existence of spatial hysteresis of the field inside the film.

Figure 6 sheds light on the transient time of approaching the reflectivity (a) and transmittivity (b) their stationary values when switching the incident field amplitude up (solid lines) and down (dotted lines), similar to that presented in Fig. 3. The calculations were done for the following parameters:  $\Psi = -\delta = 6$ ,  $\bar{N} = 30$ ,  $a = 9$ ,  $\sigma = 2$ ,  $\gamma_1 = 0.25N/\bar{N}$ ,  $\gamma = 0.875 + 0.125N/\bar{N}$ . As in the case of an ultrathin film, the transient time has the order of several units of the population relaxation time  $\bar{\Gamma}_1^{-1}$ .

In Fig. 7 we present the data of similar calculations as depicted in Fig. 4 performed for thicker films:  $L = 3\lambda_i$  and  $L = 5\lambda_i$ . As follows from these results, the hysteresis in reflection remains to be very pronounced. However, it tends to disappear in transmittivity. It is simply due to the fact that in order to make transparent a film of higher thickness, one needs to apply an input field of very high amplitude, for which the system already does not manifest at all bistability in transmission. By contrast, with regards to reflection, the film behaves as a "semi-infinite" medium, for which bistability in reflection may occur provided the parameter  $\Psi$  exceeds its critical value  $\Psi_c = 4.66$ .<sup>48</sup> In Fig. 8, we depicted the spatial profile of the field inside the film with thickness  $L = 3\lambda_i$  for the conditions for bistability to occur. It is clear from these pictures that the field is absolutely attenuated within a depth a bit longer than  $\lambda_i$  and, hence, the transmittivity in this case is negligible.

As follows from our previous study<sup>48-50</sup> of the nonlinear reflection from a collection of dense *homogeneously broadened* two-level atoms, the system may show instabilities of different types (self-oscillation and chaos) at higher values of the polariton splitting  $\Psi$ . Figure 9 presents an example of such a behavior of the film reflectivity (self-oscillation) for  $\Psi = 10$  and the *inhomogeneous broadening*  $\sigma = 2$ . The attempt to get a hysteresis loop of the reflection coefficient reveals that the lower branch is unstable (see Fig. 9a). The calculation done at a fixed amplitude of the input field ( $e_i = 8.5$ , above the switching threshold) shows that

indeed, the system has a regime of self-oscillations with a frequency of the order of  $\bar{\Gamma}/2$ .

## V. ESTIMATES OF PARAMETERS

First, let us discuss the applicability of the two-level model used in this Paper. One should compare the typical energy spacing between the first and second exciton levels  $(E_2 - E_1)/\hbar\bar{\Gamma} \simeq 3\pi^2(U/\hbar\bar{\Gamma})/\bar{N}^2$  with the switching magnitude of the input field  $e_i$ . For the parameters at hand, the former quantity ranges within the interval [3.3, 33] while the latter is approximately equal to 3. Therefore, we can conclude that our approach is correct and there is no necessity to include the one-to-two exciton transitions.

It is worthwhile to analyze the parameters of real systems in order to get insight into feasibility of the bistable mechanism we are dealing with. In this sense, the J-aggregates of PIC, as one of the most studied species of the type we need, seem to be suitable objects. The width of the red J-band of PIC-Br (centered at  $\lambda = 576.1$  nm), at low temperature, has an inhomogeneous nature and an order of magnitude of  $30\text{cm}^{-1}$  (or  $1\text{ps}^{-1}$  in frequency units)<sup>3-5</sup>. The blue shift of the transition from one-to-two exciton bands with respect to that from the ground state to the one-exciton band for the red J-band has the same order. The polariton splitting is  $\Psi\Gamma = 2\pi\bar{d}^2n_0/\hbar = (3/16\pi^2)\gamma_0\bar{N}n_0\lambda^3$ , so that taking  $\gamma_0 = (1/3.7)\text{ns}^{-1}$  and  $\bar{N}n_0 = 10^{18}\text{cm}^{-3}$  (an achievable concentration of molecules before aggregation), we obtain  $\Psi\Gamma \simeq 1\text{ps}^{-1}$ , i.e., a value that exceeds twice the halfwidth of the J-band  $0.5\text{ps}^{-1}$  ( $\sigma\Gamma$  in our notation). Hence, for the parameters used, we are under the conditions needed for bistability to occur.

## VI. CONCLUSIONS AND REMARKS

In this Paper, we have numerically studied the optical bistable response of a thin film with thickness of the order of and larger than the emission wavelength, comprised of oriented linear Frenkel chains. We have taken into account a distribution of chains over length,

resulting in an inhomogeneous broadening of the exciton optical transition as well as in the distribution of the transition dipole moment.

From our study, the following conclusions can be drawn:

(i) Within a certain range of driving parameters (resonance detuning, polariton splitting, and inhomogeneous width), the films of thickness of the order of the vacuum emission wavelength really show a bistable behavior with respect to both the reflection and transmission of the resonant light;

(ii) The bistability effect exists until the inhomogeneous width of the transition approaches the polariton splitting, i.e., for a fairly wide range of widths;

(iii) With increasing the film thickness, the bistability in the transmitted signal tends to disappear while it remains in the reflected signal;

(iv) At higher magnitude of the linear refraction index, the film reflectivity shows instabilities which are of self-oscillating type;

(v) The parameters needed for the bistable behavior seem to be achievable for a thin film of J-aggregates of polymethine dyes and for some classes of conjugated polymers deposited onto a dielectric substrate such as poly(*p*-phenylene-vinylene) derivatives.

The inhomogeneous broadening acts as a destructive factor. Reducing any source of inhomogeneity is thus of great importance. In this sense, thin films comprised of thiophene oligomers seem to be very attractive objects, too, due to the possibility of precise controlling the sizes of this type of molecules.<sup>55–58</sup>

To conclude, it is to be noted that the authors of Ref. 59 reported a room-temperature formation of polariton states in ordered cyanine dye films. The latter thus can also be considered as a promising object from the viewpoint of our findings.

## ACKNOWLEDGMENTS

V. A. M. acknowledges a partial support from INTAS (project No. 97-10434). E. C. J. acknowledges support by the Spanish Dirección General de Enseñanza Superior e Investi-

gación Científica (grant PB98-0268) and by the Junta de Castilla y León in collaboration with European Union, F. S. E. (grant SA44/01).

## REFERENCES

- <sup>1</sup> E. E. Jelley, *Nature (London)* **138**, 1009 (1936).
- <sup>2</sup> G. Scheibe, *Angew. Chem.* **50**, 51 (1937).
- <sup>3</sup> S. de Boer and D. A. Wiersma, *Chem. Phys. Lett.* **165**, 45 (1990).
- <sup>4</sup> H. Fidder, J. Knoester, and D. A. Wiersma, *Chem. Phys. Lett.* **171**, 529 (1990).
- <sup>5</sup> H. Fidder, J. Terpstra, and D. A. Wiersma, *J. Chem. Phys.* **94**, 6895 (1991).
- <sup>6</sup> F. C. Spano and J. Knoester, in *Advances in Magnetic and Optical Resonance*, Vol. **18**, ed. W. S. Warren (Academic, New York, 1994), p. 117.
- <sup>7</sup> T. Kobayashi (Ed.), *J-aggregates*, World Scientific, Singapur, 1996.
- <sup>8</sup> N. Tessler, G. J. Denton, and R. H. Friend, *Nature (London)* **382**, 695 (1996).
- <sup>9</sup> F. Hide, B. J. Schwartz, M. A. Diaz-Garsia, and A. J. Heeger, *Chem. Phys. Lett.* **256**, 424 (1996).
- <sup>10</sup> S. V. Frolov, W. Gellermann, M. Ozaki, K. Yoshino, and Z. V. Vardeny, *Phys. Rev. Lett.* **78**, 729 (1997).
- <sup>11</sup> S. V. Frolov, Z. V. Vardeny, and K. Yoshino, *Phys. Rev. B* **57**, 9141 (1998).
- <sup>12</sup> S. Özçelik and D. L. Akins, *Appl. Phys. Lett.* **71**, 3057 (1997).
- <sup>13</sup> S. Özçelik, I. Özçelik, and D. L. Akins, *Appl. Phys. Lett.* **73**, 1949 (1998).
- <sup>14</sup> D. G. Lizdey, D. D. C. Bradley, T. Virgili, A. Armitage, and M. S. Scolnik, *Phys. Rev. Lett.* **82**, 3316 (1999).
- <sup>15</sup> N. Tessler, *Adv. Mater.* **11**, 363 (1999).
- <sup>16</sup> G. Kranzelbinder and G. Leising, *Rep. Prog. Phys.* **63**, 729 (2000).
- <sup>17</sup> M. D. McGehee and A. J. Heeger, *Adv. Mater.* **12**, 1655 (2000).

- <sup>18</sup> S. M. Zakharov and E. A. Manykin, *Poverkhnost'* **2**, 137 (1988).
- <sup>19</sup> A. M. Basharov, *Zh. Exp. Teor. Fiz.* **94**, 12 (1988) [*JETP* **67**, 1741 (1988)].
- <sup>20</sup> M. G. Benedict, A. I. Zaitsev, V. A. Malyshev, and E. D. Trifonov, *Opt. Spektrosk.* **68**, 812 (1990) [*Opt. Spectrosc.* **68** 473 (1990)].
- <sup>21</sup> M. G. Benedict, V. A. Malyshev, E. D. Trifonov, and A. I. Zaitsev, *Phys. Rev. A* **43**, 3845 (1991).
- <sup>22</sup> M. G. Benedict, A. M. Ermolaev, V. A. Malyshev, I. V. Sokolov, and E. D. Trifonov, *Super-radiance: Multiatomic coherent emission* (Bristol and Philadelphia: Institut of Physics Publishing, 1996).
- <sup>23</sup> Yu. A. Logvin and A. M. Samson, *Opt. Commun.* **96**, 107 (1993).
- <sup>24</sup> V. V. Gusev, *Adv. Mater. Opt. Electr.* **1**, 235 (1992).
- <sup>25</sup> V. Malyshev and P. Moreno, *Phys. Rev. A* **53**, 416 (1996).
- <sup>26</sup> V. A. Malyshev, H. Glaeske and K.-H. Feller, *Opt. Commun.* **140**, 83 (1997); *J. Lumin.* **76&77**, 445 (1998);
- <sup>27</sup> V. A. Malyshev, H. Glaeske and K.-H. Feller, *Phys. Rev. A* **58**, 670 (1998).
- <sup>28</sup> J. Heber, *Z. Phys. B* **68**, 115 (1987).
- <sup>29</sup> N. Bodenschatz and J. Heber, *Phys. Rev. A* **54**, 4428 (1996).
- <sup>30</sup> V. A. Malyshev, H. Glaeske and K.-H. Feller, *Phys. Rev. A* **58**, 1496 (1998).
- <sup>31</sup> E. W. Knapp, *Chem. Phys.* **85**, 73 (1984).
- <sup>32</sup> V. I. Bogdanov, E. N. Viktorova, S. V. Kulya, and A. S. Spiro, *Pis'ma Zh. Eksp. Teor. Fiz.* **53**, 100 (1991)[*JETP Lett.* **53**, 105 (1991)].
- <sup>33</sup> Y. Wang, *J. Opt. Soc. Am. B* **8**, 981 (1991).

- <sup>34</sup> K. Minoshima, M. Taiji, K. Misawa, T. Kobayashi, Chem. Phys. Lett. **218** 67 (1994).
- <sup>35</sup> E. O. Potma and D. A. Wiersma, J. Chem. Phys. **108**, 4894 (1998).
- <sup>36</sup> V. A. Malyshev, H. Glaeske and K.-H. Feller, Opt. Commun. **169**, 177 (1999); J. Lumin. **83-84**, 291 (1999); J. Chem. Phys. **113**, 1170 (2000).
- <sup>37</sup> V. A. Malyshev, Opt. Spektrosk. **71**,873 (1991) [Opt. Spectrosc. **71**, 505 (1991)]; J. Lumin. **55**, 225 (1993).
- <sup>38</sup> V. Malyshev and P. Moreno, Phys. Rev. B **51**, 14 587 (1995).
- <sup>39</sup> In Ref. 36, only the fluctuations of the one-exciton transition frequency (inhomogeneous broadening) have been taken into account.
- <sup>40</sup> V. A. Malyshev and E. Conejero Jarque, Opt. Exp. **6**, 227 (2000).
- <sup>41</sup> D. B. Chesnut and A. Suna, J. Chem. Phys. **39**, 146 (1963).
- <sup>42</sup> H. Fidder, J. Knoester and D. A. Wiersma, J. Chem. Phys. **98**, 6564 (1993).
- <sup>43</sup> H. Glaeske, V. A. Malyshev, and K.-H. Feller, J. Chem. Phys. **114**, 1966 (2001).
- <sup>44</sup> V. A. Malyshev, H. Glaeske and K.-H. Feller, Chem. Phys. Lett. **305**, 117 (1999); Chem. Phys. **254**, 31 (2000).
- <sup>45</sup> Such conditions are achievable for thin films prepared by the spin coating method<sup>46</sup>.
- <sup>46</sup> K. Misawa, K. Minoshima, H. Ono, and T. Kobayashi, Appl. Phys. Lett. **63**, 577 (1993).
- <sup>47</sup> M. G. Benedict and E. D. Trifonov, Phys. Rev. A **38** (1988) 2854.
- <sup>48</sup> V. A. Malyshev and E. Conejero Jarque, J. Opt. Soc. Am. B **12** (1995) 1868; J. Lumin. **72-74** (1997) 822; Opt. Spektr. **82** (1997) 630 [Opt. Spectr. **82** (1997) 582].
- <sup>49</sup> V. A. Malyshev and E. Conejero Jarque, J. Opt. Soc. Am. B **14** (1997) 1167.
- <sup>50</sup> E. Conejero Jarque and V. A. Malyshev, Opt. Commun. **142** (1997) 66.

- <sup>51</sup> J. T. Manassah and B. Gross, *Opt. Commun.* **131** (1996) 408; *ibid.* **148** (1998) 404; *ibid.* **149** (1998) 393; *ibid.* **155** (1998) 213.
- <sup>52</sup> L. Roso-Franco, *Phys. Rev. Lett.* **55** (1985) 2149; *J. Opt. Soc. Am. B* **4** (1987) 1878.
- <sup>53</sup> L. Roso-Franco and M. Ll. Pons, *J. Mod. Opt.* **37** (1990) 1645.
- <sup>54</sup> A. S. Davydov, *Theory of molecular excitons*, Plenum Press, New York, 1971.
- <sup>55</sup> P. Ostoja, S. Guerri, S. Rossini, M. Servidory, C. Taliani, and R. Zamboni, *Synth. Met.* **54**, 447 (1993).
- <sup>56</sup> B. Servet, S. Ries, M. Tritel, P. Alnot, G. Horowitz, and H. Garnier, *Adv. Mater.* **5**, 461 (1993).
- <sup>57</sup> L. M. Blinov, S. P. Palto, G. Ruani, C. Taliani, A. A. Tevosov, S. G. Yudin, and R. Zamboni, *Chem Phys. Lett.* **232**, 401 (1995).
- <sup>58</sup> F. Garnier, G. Horowitz, P. Valat, and F. Kouki, *Appl. Phys. Lett.* **72**, 2087 (1998).
- <sup>59</sup> L. Daehne and E. Biller, *Phys. Chem. Chem. Phys.* **1**, 1727 (1999).



## FIGURES

FIG. 1.  $(\sigma, \psi)$ -map obtained by solving Eq. (10). The solid line separates two regions within which there are one and three real solutions of Eq. (10) and thus represents the critical value of  $\psi$  for bistability to occur versus the inhomogeneous width  $\sigma = 2\pi^2 U a / \hbar \bar{\Gamma} \bar{N}^3$ . The dashed line is calculated under the assumption that  $\delta$  is the only stochastic parameter, as was done in Ref. 36.

FIG. 2. Amplitude reflection (a) and transmission (b) coefficients of an ultrathin film ( $k_i L = 0.1$ ) calculated using Eqs. (7) with the input field amplitude  $e_i = \bar{d}E_i / \hbar \bar{\Gamma}$  scanned up and down for different values of  $\sigma = 2\pi^2 U a / \hbar \bar{\Gamma} \bar{N}^3$  where  $U / \hbar \bar{\Gamma}$  was varied. Other parameters were chosen as follows:  $\psi = 20$ ,  $\bar{N} = 30$ ,  $a = 9$ ,  $\gamma_1 = 0.25N / \bar{N}$ ,  $\gamma = 0.875 + 0.125N / \bar{N}$ . Time is in units of  $\bar{\Gamma}^{-1}$ .

FIG. 3. Kinetics of approaching the reflection (a) and transmission (b) coefficients their stationary values after a sudden switching (at an instant  $\tau = \bar{\Gamma}t = 50$ ) of the incident field amplitude. The calculations were done for the parameters of Fig. 2 setting  $\sigma = 0.25$ . The solid lines represent the results obtained when the input field amplitude was switched from a low value  $e_i = \bar{d}E_i / \hbar \bar{\Gamma} = 3$  (a high reflection) to a higher value  $e_i = \bar{d}E_i / \hbar \bar{\Gamma} = 6$  (a low reflection). The dotted lines represent the results for the back switching of the input field amplitude, from  $e_i = 6$  to  $e_i = 3$ . Time is in units of  $\bar{\Gamma}^{-1}$ .

FIG. 4. The amplitude reflection ( $\mathcal{R}$ ) and transmission ( $\mathcal{T}$ ) coefficients of a film with thickness  $L = \lambda_i$  ( $k_i L = 2\pi$ ) calculated at adiabatic scanning of the input field amplitude  $e_i = \bar{d}E_i / \hbar \bar{\Gamma}$  up and down for different values of the inhomogeneous width  $\sigma = 2\pi^2 U a / \hbar \bar{\Gamma} \bar{N}^3$ , where  $U / \hbar \bar{\Gamma}$  was varied. Other parameters were chosen as follows:  $\Psi = 2\pi \bar{d}^2 n_0 / \hbar \bar{\Gamma} = -\delta = 6$ ,  $\gamma_1 = 0.25N / \bar{N}$ ,  $\gamma = 0.875 + 0.125N / \bar{N}$ . Time is in units of  $\bar{\Gamma}^{-1}$ .

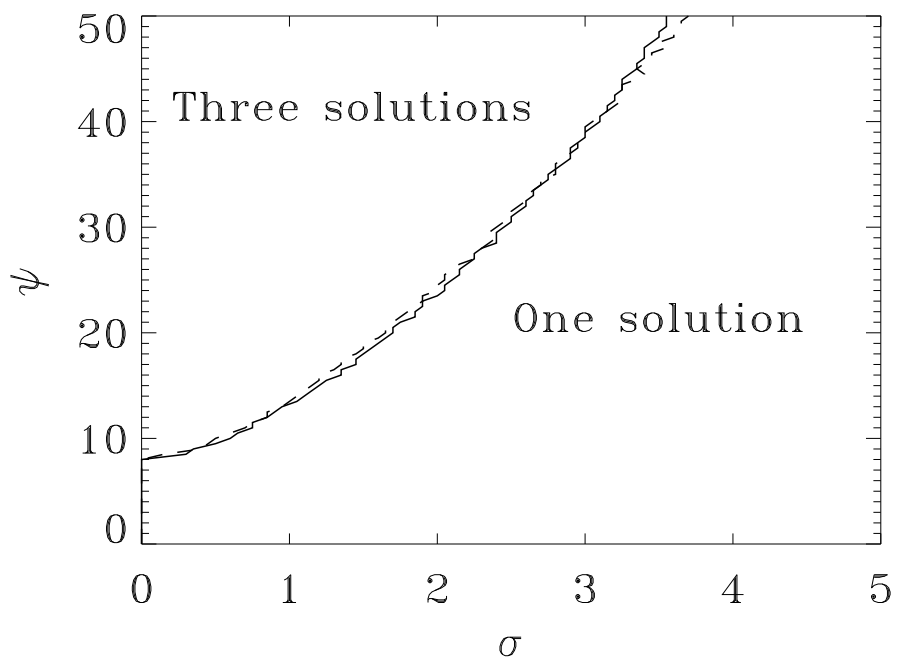
FIG. 5. Examples of the spatial profiles of the field amplitude module inside the film corresponding to the case with  $\sigma = 2$  in Fig. 4. The graphs (a) and (b) show the inside field profiles when the input field amplitude  $e_i = \bar{d}E_i / \hbar \bar{\Gamma}$  is scanned up and down, respectively. The darkness of a local differential domain is proportional to the module of the inside field amplitude,  $|e| = \bar{d}|E| / \hbar \bar{\Gamma}$ .

FIG. 6. Kinetics of approaching the reflection (a) and transmission (b) coefficients their stationary values, calculated after a sudden switching (at an instant  $\tau = \bar{\Gamma}t = 50$ ) of the input field amplitude from a value  $e_i = \bar{d}E_i/\hbar\bar{\Gamma} = 2$  below the switching point  $e_i \approx 2.9$  to a one  $e_i = \bar{d}E_i/\hbar\bar{\Gamma} = 3.5$  above the latter (solid line). By the dotted line, the back switching is shown. The parameters are the same as in Fig. 5. Time is in units of  $\bar{\Gamma}^{-1}$ .

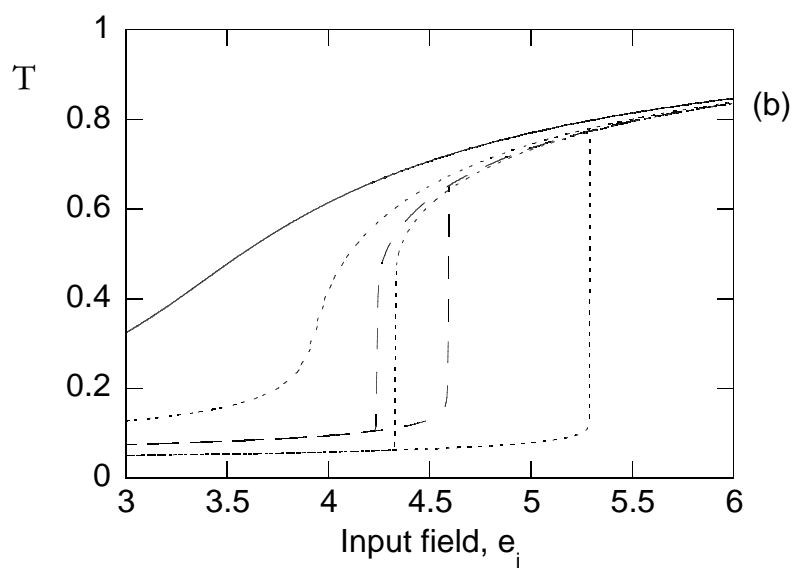
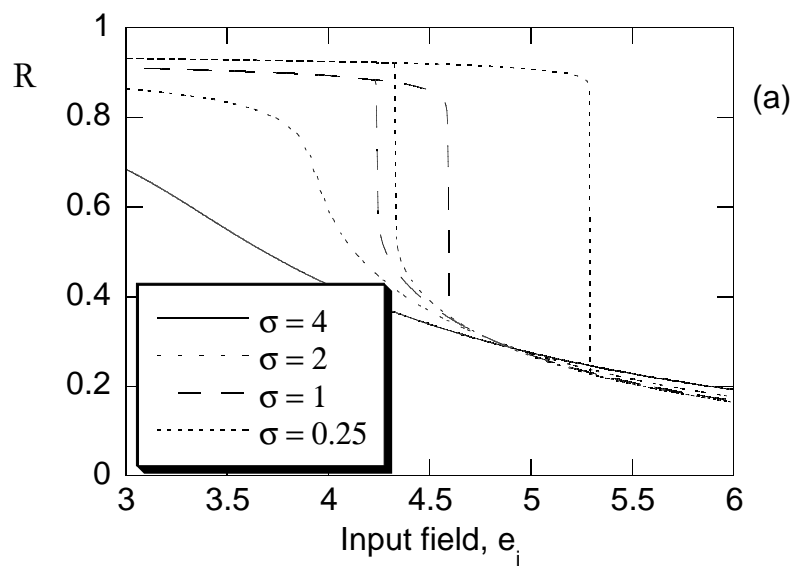
FIG. 7. The same as in Fig. 4 (a) for the case of  $\sigma = 2$  and several values of the slab thickness.

FIG. 8. The same as in Fig. 5 for a slab of thickness  $L = 3\lambda_i$ .

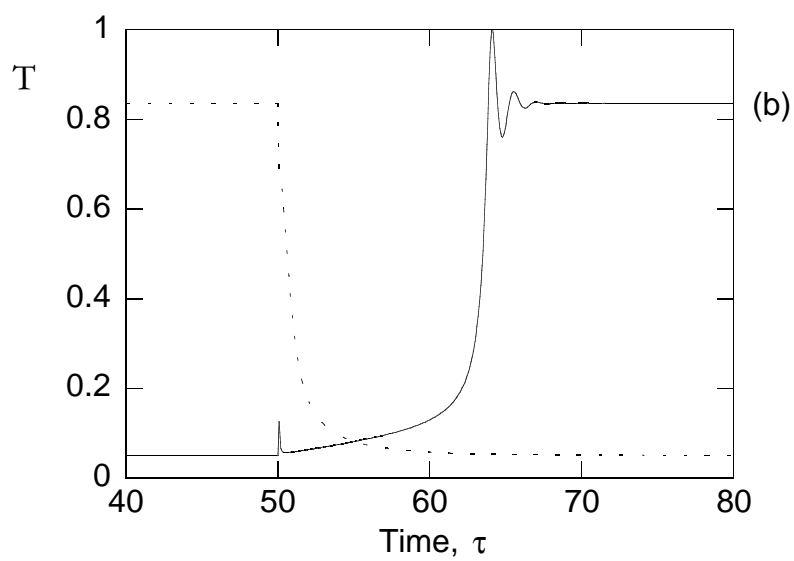
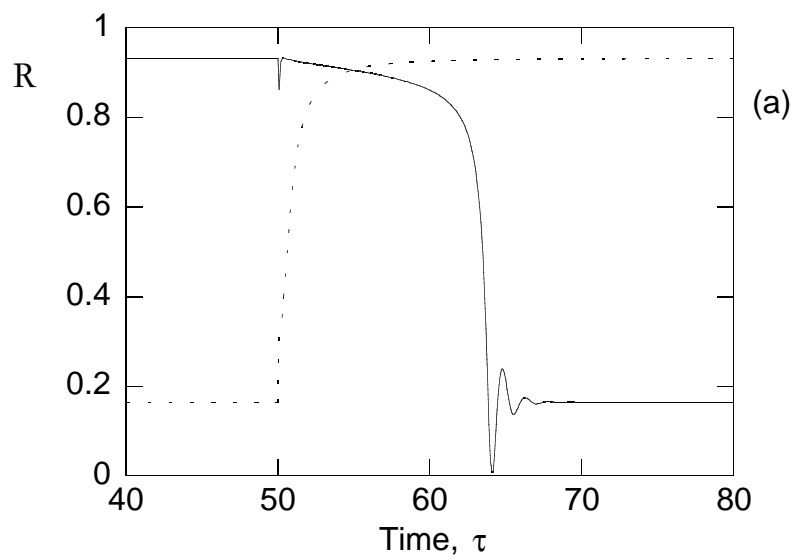
FIG. 9. a - Optical hysteresis loop of the reflection coefficient for a film of thickness  $L = 2\lambda_i$  revealing an instability. The calculation was done by means of Eqs. (7) at adiabatic scanning of the input field amplitude  $e_i = \bar{d}E_i/\hbar\bar{\Gamma}$  up and down, setting the following parameters:  $\Psi = 10 = -\delta$ ,  $\bar{N} = 30, a = 9, \sigma = 2, \gamma_1 = 0.75N/\bar{N}, \gamma = 0.625 + 0.375(N/\bar{N})$ . b - Kinetics of the reflection coefficient  $\mathcal{R}$  calculated at a fixed amplitude of the input field ( $e_i = 8.5$ ) showing self-oscillations. The set of parameters is the same as in plot a. Time is in units of  $\bar{\Gamma}^{-1}$ .



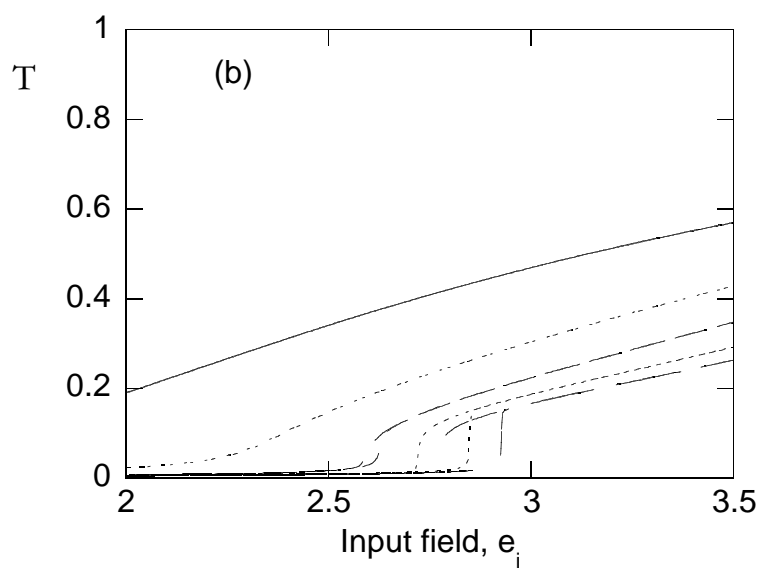
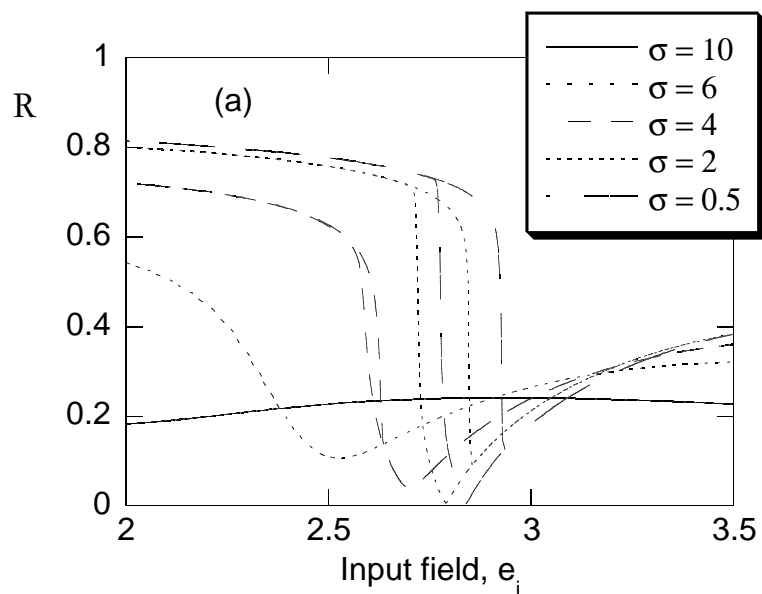
Conejero Jarque, J. Chem. Phys., Figure 1



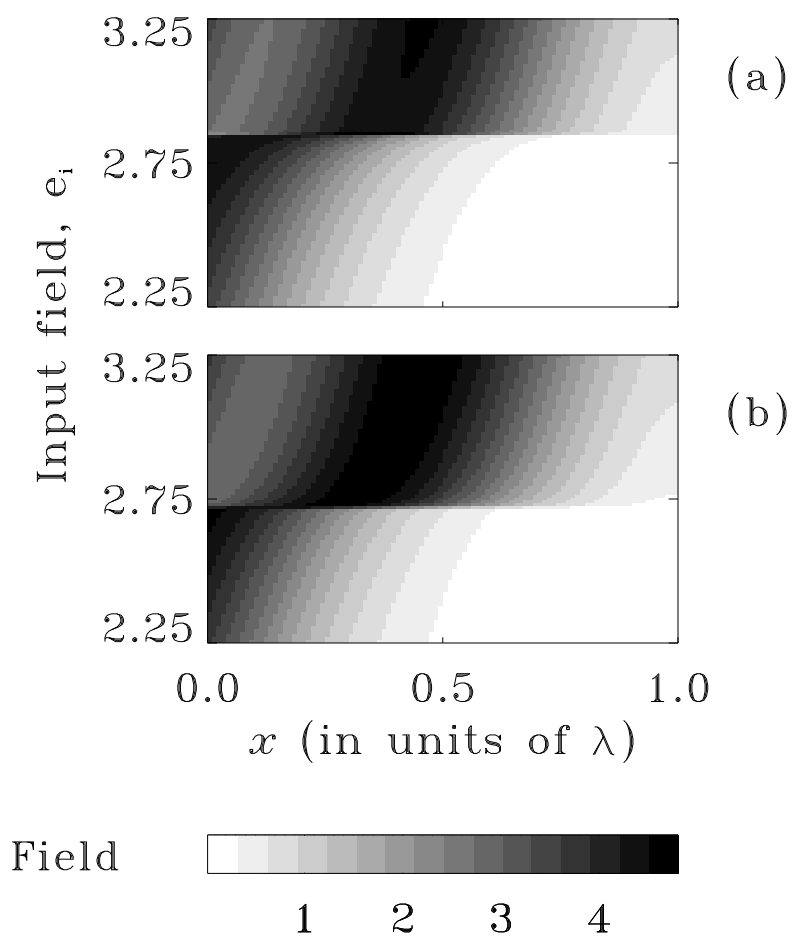
Conejero Jarque, J. Chem. Phys., Figure 2



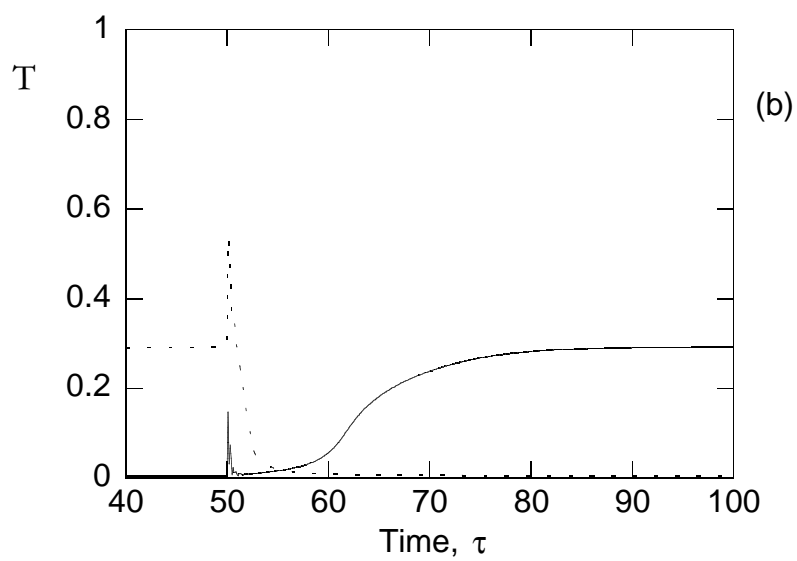
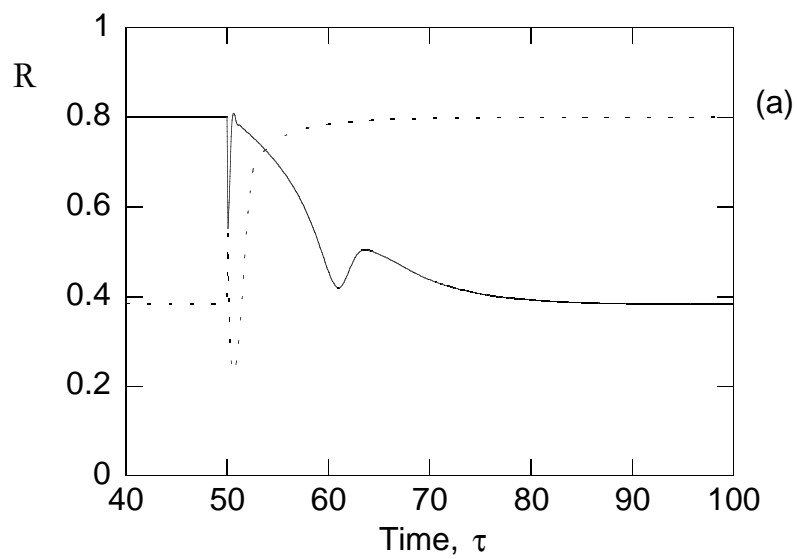
Conejero Jarque, J. Chem. Phys., Figure 3



Conejero Jarque, J. Chem. Phys., Figure 4

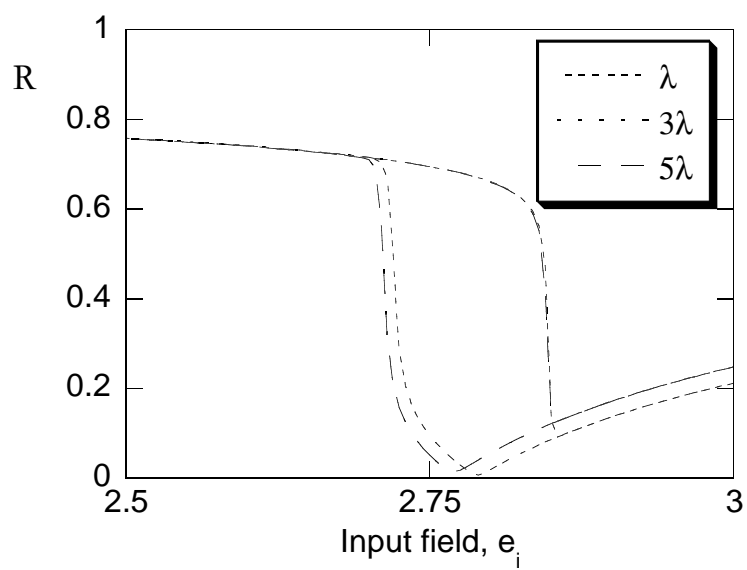


Conejero Jarque, J. Chem. Phys., Figure 5

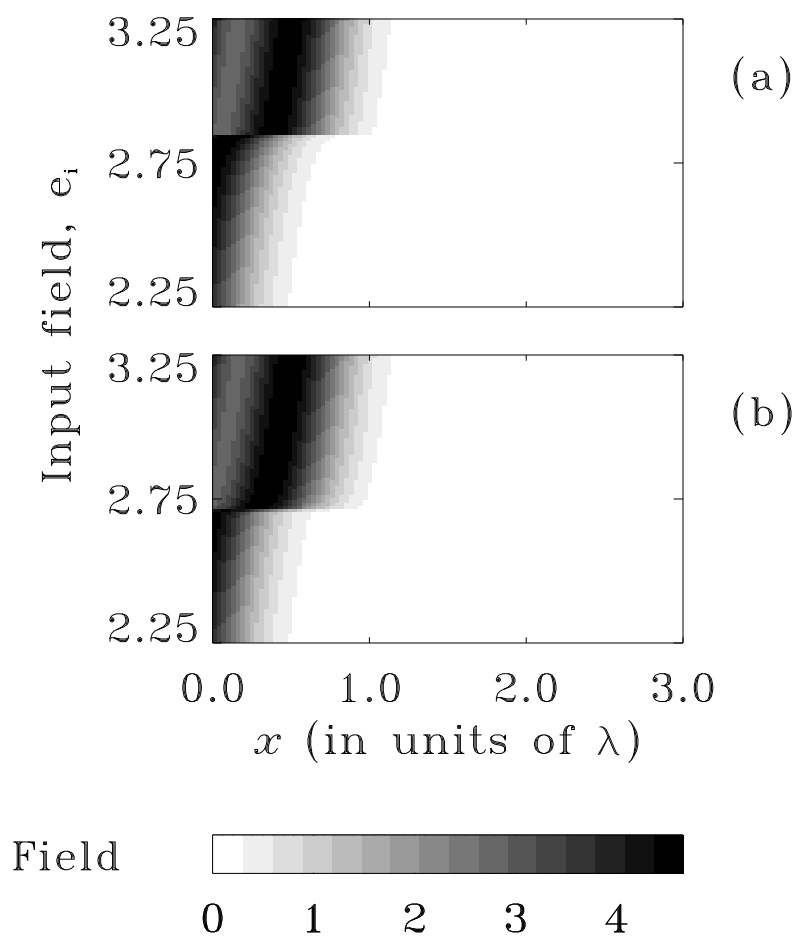


Conejero Jarque, J. Chem. Phys., Figure 6

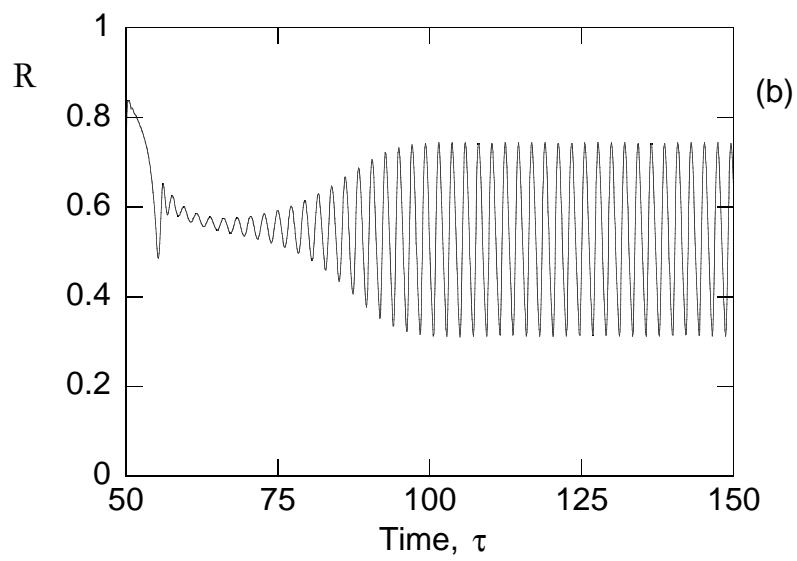
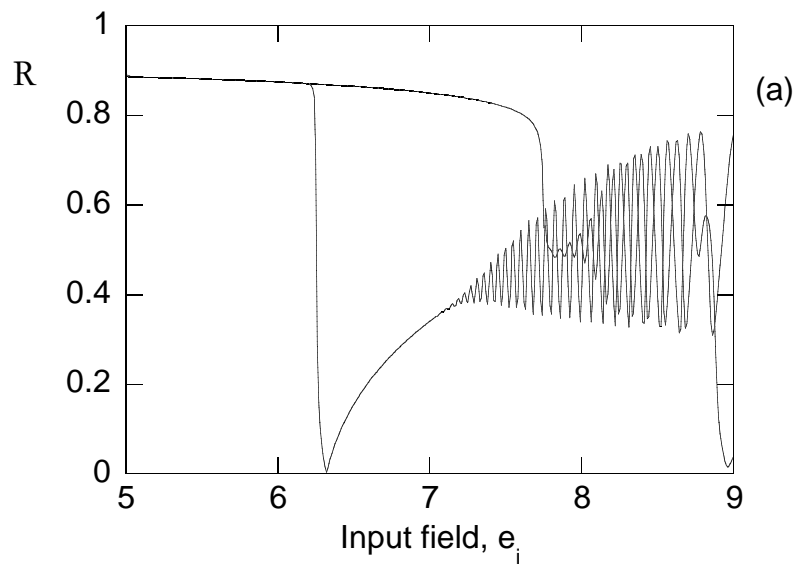




Conejero Jarque, J. Chem. Phys., Figure 7



Conejero Jarque, J. Chem. Phys., Figure 8



Conejero Jarque, J. Chem. Phys., Figure 9